Lab on a Chip

Cite this: *Lab Chip*, 2012, **12**, 2656–2663

www.rsc.org/loc

PAPER

A microfluidic "baby machine" for cell synchronization†

Josephine Shaw,[a] Kristofor Payer,[b] Sungmin Son,[c] William H. Grover[a] and Scott R. Manalis*[acd]

Received 19th March 2012, Accepted 20th April 2012
DOI: 10.1039/c2lc40277g

Common techniques used to synchronize eukaryotic cells in the cell cycle often impose metabolic stress on the cells or physically select for size rather than age. To address these deficiencies, a minimally perturbing method known as the "baby machine" was developed previously. In the technique, suspension cells are attached to a membrane, and as the cells divide, the newborn cells are eluted to produce a synchronous population of cells in the G1 phase of the cell cycle. However, the existing "baby machine" is only suitable for cells which can be chemically attached to a surface. Here, we present a microfluidic "baby machine" in which cells are held onto a surface by pressure differences rather than chemical attachment. As a result, our method can in principle be used to synchronize a variety of cell types, including cells which may have weak or unknown surface attachment chemistries. We validate our microfluidic "baby machine" by using it to produce a synchronous population of newborn L1210 mouse lymphocytic leukemia cells in G1 phase.

Introduction

Synchronization of cells in the cell cycle is imperative in the study of many cellular and molecular processes. It specifically allows for the study of molecular regulatory mechanisms and genetic expression throughout the cell cycle, which has facilitated the discovery of biomarkers for cancer prognosis and drug development.[1–3] In addition, since cells have different molecular compositions and distinct responses to stimuli while in different phases of the cell cycle, synchronization methods are used to reduce biological noise in experiments involving populations of cells.

The most common techniques for synchronizing eukaryotic cells involve the addition or depletion of certain compounds that stall the cells at a particular phase in the cell cycle. The cells are then released to continue progression of the division cycle by the removal of the drug or re-addition of growth factors. For example, in serum starvation, removing serum from a growing culture can cause the cells to enter a quiescent state, and upon the reintroduction of serum, the cells re-enter the cell division cycle. However, serum starvation has been found to reduce cell survival and increase DNA fragmentation, and re-entry into the cell cycle is often not synchronous.[4,5] Similarly, DNA synthesis inhibitors such as excess thymidine and hydroxyurea stall cells in S phase, while microtubule polymerization inhibitors such as nocodazole and colcemid stall cells in mitosis.[6] Nonetheless, such compounds have unwanted side-effects, including activating the DNA damage response, influencing RNA synthesis, and inducing apoptosis, especially at higher concentrations.[7–11] Although these batch chemical methods may align cells to a certain feature of the cell cycle, it is known that such drugs perturb the growth and progression of internal molecular machinery. For instance, even while DNA synthesis is inhibited, other cellular processes such as transcription and translation still continue, creating a growth imbalance in the cell.[12] Thus, mitotic and replication inhibitors place cells in nonphysiological states, and even though synchronization with them may be valid for some experiments, the extent of their usefulness may be limited.[5,13–15] The resulting growth imbalance may particularly confound studies regarding cell growth, metabolism, and their relation to the cell cycle. Indeed, it has even been found that protein expression in chemically synchronized cells does not match that of unperturbed cells.[16] Hence, the applicability of results from cells obtained by batch chemical methods to normal, unperturbed cells remains questionable.

Another common way to synchronize cells is physically extracting a subpopulation of cells with similar properties, rather than coercing the entire culture to converge at the chosen characteristic. One such technique is counterflow centrifugal elutriation, which uses centrifugal force balanced by a centripetal flow of fluid in a specially designed centrifuge rotor to separate the cells by their sedimentation velocity, which is dependent upon cell size and shape.[17–19] Although this method successfully isolates different sizes of cells, with the smallest cells assumed to be in G1 phase, it exposes them to harsh conditions, such as a 683 × *g* rotor speed at 20 °C for 4–5 h.[19] More recently, cells have been separated by size in microfluidic devices using

[a]*Department of Biological Engineering, Massachusetts Institute of Technology, Cambridge, MA, USA*
[b]*Microsystems Technology Laboratories, Massachusetts Institute of Technology, Cambridge, MA, USA*
[c]*Department of Mechanical Engineering, Massachusetts Institute of Technology, Cambridge, MA, USA. E-mail: scottm@media.mit.edu*
[d]*Koch Institute for Integrative Cancer Research, Massachusetts Institute of Technology, Cambridge, MA, USA*
† Electronic supplementary information (ESI) available. See DOI: 10.1039/c2lc40277g

dielectrophoresis, acoustophoresis, hydrophoresis, hydrodynamic filtration, or inertial forces.[20–24] However, the size of the cell does not necessarily indicate its age, so the resulting similarly-sized cells may still have a range of ages due to inherent biological variation. Cells may also be sorted based upon DNA content using flow cytometry, but the use of DNA-staining dyes may cause mutagenicity and affect cell viability.[6,12] Furthermore, a synchronous batch of G1 cells selected based on DNA content rather than a particular event in the cell cycle could have an age range spanning the length of G1, which can occupy over 40% of the eukaryotic cell cycle, depending on the cell type.[25] In addition, both centrifugal elutriation and flow cytometry require costly equipment.

A simpler and less perturbing method for synchronizing cells is mitotic shake-off. Adherent cells that grow in a monolayer culture often become spherical during mitosis, at which point they can be detached by shaking or agitation. Since mitosis comprises only a short portion of the cell cycle, sometimes the shake-off method is used in conjunction with chemical synchronization methods to increase yields; this introduces the same concerns mentioned previously with chemical techniques.[7,26,27] Moreover, the mitotic shake-off method is only possible for adherent, monolayer cell cultures.[6,12]

In the 1960s, Helmstetter *et al.* developed the membrane elution method of synchronization, colloquially known as the "baby machine".[28] In this method, cells are bound to a membrane, and as they divide, one cell remains adhered while the other is eluted. This yields a population of cells synchronized at the beginning of G1 phase. The technique was first used with bacteria, and was later customized for mammalian cells in 2002 and improved upon in 2006.[28–30] Although the "baby machine" is arguably the least perturbing method of cell synchronization, it has not been widely adopted. Furthermore, the technique depends on the ability of cells to bind to membranes coated with concanavalin A, poly-D-lysine, *etc.*[29] Cells with weak or unknown binding ability would thus be difficult or impossible to synchronize using the "baby machine".

Here we present a technique in which a pressure differential is used to adhere thousands of cells to a surface, while allowing for constant perfusion of culture medium as well as elution of newborn cells. This technique requires no specific cell surface chemistry and should be amenable to virtually any suspension cell type. As a proof-of-principle, we fabricated and tested microfluidic devices that include an array of 2 μm diameter trapping holes onto which cells can be loaded. We demonstrate that L1210 mouse lymphocytic leukemia cells load into the device, grow and divide on chip, and elute a synchronous population of cells in G1 phase.

Materials and methods

Device description

The silicon and glass microfluidic "baby machine" consists of an introduction channel that is bifurcated twice and feeds into the main cell capture chamber. This chamber is 4 mm wide and 5 mm long, and houses 2109 trapping holes onto which cells can be captured (Fig. 1a). The holes are staggered and spaced 45 μm from one another, and are placed at least 1.75 mm away from the entrances and exits of the chamber to allow a uniform flow profile to develop. The dimensions and spacing were chosen to minimize the variation in pressures and stresses experienced by the cells in different regions of the capture chamber. The small pressure drop horizontally across the chamber also allows the vertical trapping pressures to be relatively uniform and sensitively controlled for optimal operation.

Four access ports provide fluidic access to the device: inlet, bypass, backside, and outlet. The inlet is where fluid is introduced, the bypass allows for quick rinsing away of excess cells, the backside enables control of the vertical pressure drop across the trapping holes, and the outlet is where the eluted newborn cells are collected. An external fluid valve placed in-line with the bypass tubing is opened during rinsing and closed during perfusion. Although separate pressure regulators can manipulate the pressure at each port, we found that successful operation of the device could be achieved by using only one regulator at the inlet, while leaving the other ports at atmospheric pressure. Finer pressure balances were achieved by adjusting tubing resistances and fluid levels in the vials. These fine-tuned parameters generally remain unchanged from one experiment to the next.

Device fabrication

The devices were fabricated using standard silicon and glass microfabrication techniques. The top layer consists of a 500 μm thick, 6 inch glass wafer (Bullen), with fluidic channels etched into it at two depths: 80 μm for the cell capture chamber and 30 μm for all other channels. The bottom of the device is a 6 inch silicon on insulator (SOI) wafer (Ultrasil Corporation), having a 15 μm device layer and a 0.5–2 μm thick buried oxide layer. The 2 μm diameter trapping holes as well as the fluidic access ports were etched through the device layer using deep reactive ion etching (DRIE). After patterning the backside, the SOI was mounted onto a dummy wafer and DRIE was used to etch a reservoir below the trapping holes and open up the fluidic access ports from the bottom. The exposed oxide was then stripped in 25% HF to fully release the trapping holes and fluidic access ports. Finally, the glass and silicon wafers were anodically bonded.

System assembly

The silicon–glass device is set in a polytetrafluoroethylene (PTFE) gasket with perfluoroelastomer o-rings, while the entire setting is clamped between two aluminium plates to create a fluidic seal. The aluminium plates have openings cut out for microscope viewing from above and fluidic connections from below. The aluminium clamp then resides in a copper setting that enables temperature control *via* a recirculating water bath (Thermo Scientific). In all experiments, the temperature of the device was maintained at 37 °C.

To introduce fluid into the device, computer-controlled electronic pressure regulators (Proportion Air) were used to pressurize glass vials to which the fluidic tubing was connected through PTFE septa. The tubing that connected the vials to the device were made of fluorinated ethylene propylene (IDEX Health and Science), and were of varying inner diameters (0.15–0.41 mm), chosen to balance the resistances of the fluid flow. The

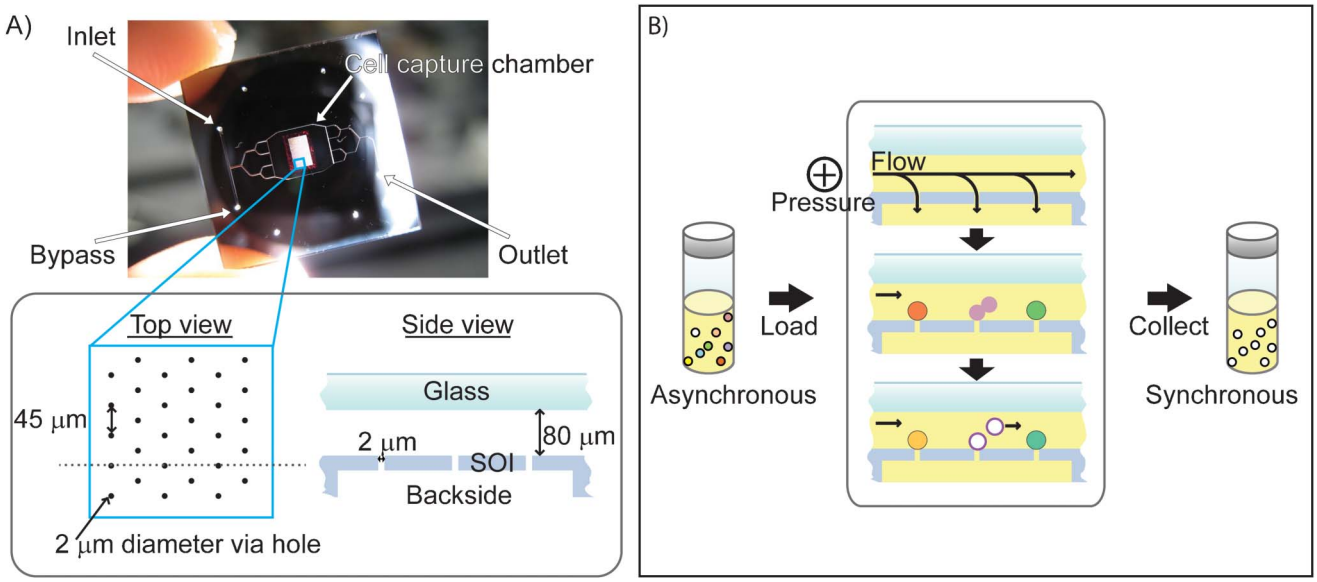

Fig. 1 (A) Image of the synchronization device illuminated from the backside, showing branching fluidic channels that lead into a cell capture chamber with 2109 2 μm diameter holes onto which cells can be loaded. In the schematic diagram, the side view is an illustration of the cross section along the dotted line in the top view. The channels are etched into the top glass wafer, and the 2 μm holes and fluidic ports are etched into the bottom SOI wafer. (B) Operation of the device is controlled entirely by pressure differences. A positive pressure applied at the inlet creates both a pressure differential in the vertical direction across the holes to capture cells, as well as a pressure drop in the horizontal direction to generate lateral flow for the collection of daughter cells. An asynchronous population of cells is fed into the device and captured onto the holes, and with a constant slow perfusion of cell culture medium, the cells grow within the device. As they divide, the newborn cells, which are not anchored to trapping holes, are carried away in the fluid flow and eluted into a collection chamber. The eluted cells then compose a synchronous population of cells that has just completed cytokinesis and entered the G1 phase of the cell division cycle.

outlet tubing was also kept short to minimize transit time for the cell to leave the device and enter the collection chamber.

Device operation

In preparation for cell synchronization, the device is first filled with ethanol to ensure flow through all of the trapping holes and to rid the system of air bubbles. Next, it is rinsed with purified, filtered water (Milli-Q) for at least one hour with an input pressure of 37 kPa; this cleans the surface and purges any remaining air bubbles. To reduce surface fouling, the channels are then treated with poly(L-lysine)-*graft*-poly(ethylene glycol) co-polymer (Surface Technology, Switzerland) at a concentration of approximately 0.5 mg mL^{-1} in phosphate buffered saline (PBS) for 30 min. The device is again rinsed with water and then primed with fresh cell culture medium at 37 °C.

Next, to load cells into the device, the pressure regulator at the inlet is set to 3.4 kPa. After the cells are loaded, fresh, pre-warmed media is placed at the inlet and the excess cells are rinsed away. Then, the pressure at the inlet is reduced to approximately 0.6 kPa; the resulting lateral flow rate perfuses nutrients to the cells while imparting a minimum amount of shear stress. Using a plane Poiseuille flow approximation in the main chamber, the highest shear stress experienced by the cells during the transient loading of the device is 0.02 Pa (0.2 dyne cm^{-2}), while the shear stress during long term perfusion is 0.003 Pa (0.03 dyne cm^{-2}); both of these values are well below physiological shear stresses.[31,32] The perfusion rate is 40 μL h^{-1} and the flow in the device is laminar (Re ≈ 0.003–0.02 in the main chamber).

To ensure that insecurely docked cells do not detach from the device and contaminate the output, the collection of cells does not begin until after over an hour of perfusion. For the experiments presented here, we collected a new fraction of cells in a fixative every 12 h to validate the count and synchrony of the output. Since the cells are fixed upon exiting the device, the synchrony of the output is maintained for the duration of cell collection. However, in an experiment where one wished to use the live, synchronized G1 cells outputted by the device, the collection duration would be dictated by the desired number of cells and degree of synchrony: a short collection would yield a smaller number of cells with very similar ages, and a longer collection would yield a larger number of cells with increased age variability. Afterwards, the device can be washed using 10% bleach or piranha (3 : 1 [v/v] H_2SO_4 : H_2O_2), rinsed thoroughly with water, and reused.

Cell count and cell cycle analysis

To assay the throughput and synchrony of the output from the device, cells were eluted into a formaldehyde fixative solution and, at 12 hour intervals, were counted and stained with DAPI. Since the fixative solution becomes more dilute as the cells elute, the initial solution contained 6% formaldehyde (Sigma-Aldrich F1635) in 1× PBS, such that the final concentration of formaldehyde after 12 h of collection would be 4%. For every 12 hour fraction of fixed output from the device, the number of cells in a 40 μL portion was counted manually using bright field microscopy. The determined concentration was then used to

extrapolate the total number of cells eluted over the 12 hour period.

After a portion of the eluted cells were counted, the rest were stained using 3 μM DAPI (Invitrogen D1306) with 0.1% Triton X-100 (Sigma-Aldrich T-8787). Following 20 min of incubation with the dye, the cell solution was centrifuged at 300 × *g* for 6 min and resuspended in 20 μL of 1× PBS. For the data presented, the cells were imaged on a glass slide using a 10× objective (Nikon, CFI Plan Fluor) on an upright Nikon microscope. To validate this method, replicate experiments were imaged using deconvolution fluorescence microscopy (enhanced additive method) with a 20× objective (Olympus, UApo340) on an Applied Precision DeltaVision Spectris Imaging System, which yielded similar results (not shown).[33] The process of obtaining the fluorescence intensities of the cells in each image was automated using a macro script for ImageJ. The results were then analyzed using scripts written in MATLAB and further validated manually to ensure that only cells, and not dust or debris, were being used as data.

Cell culture

L1210 mouse lymphocytic leukemia cells were cultured in Leibovitz L-15 medium (Invitrogen 21083027) supplemented with 10% fetal bovine serum (Invitrogen 16000), 0.4% glucose (Sigma-Aldrich G8769) and 1% penicillin/streptomycin (Invitrogen 151400). They were grown in 25 cm^2 culture flasks at 37 °C in an atmosphere containing 5% carbon dioxide. Cells were seeded at a concentration of around 5×10^4 cells mL^{-1} and diluted into fresh medium every two days. The concentration of cells used during experiments was between 2×10^5 and 4×10^5 cells mL^{-1}.

Results and discussion

Working principles

The synchronization device is designed such that pressures alone control both the adherence of cells onto the device and the elution of G1 cells out from the device. Similar to the original "baby machine", an asynchronous population of cells is loaded into the device, and a synchronous population of newborn cells is collected at the outlet. However, as shown in Fig. 1b, instead of using surface chemistries to trap cells, the microfluidic "baby machine" captures cells by the application of a vertical pressure differential across 2 μm diameter trapping holes. With a constant slow perfusion of cell culture medium in the horizontal direction, the cells grow within the device. When the cells divide, the newborn cells that are not anchored to a trapping hole are carried away by the fluid flow and eluted into a collection chamber. The eluted cells compose a synchronous population of cells that has just completed cytokinesis and has entered the G1 phase of the cell division cycle.

Cell loading and viability

We first verified that the cells could be loaded onto the trapping holes without being squeezed through or sheared off of them during the constant perfusion of culture medium. L1210 cells were introduced into the device and observed *via* microscopy. Bright field images (Fig. 2a) show that the cells can indeed fill the

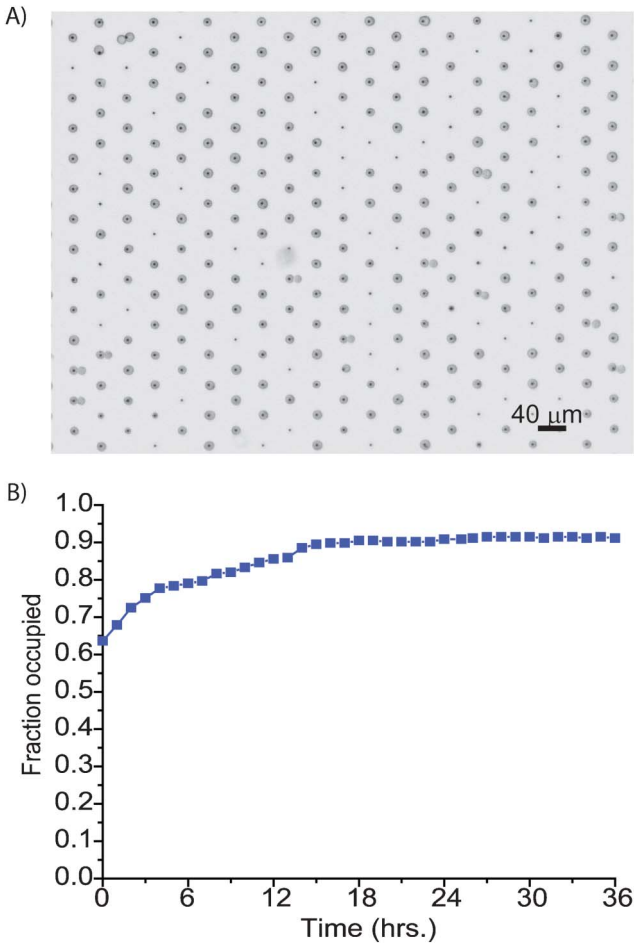

Fig. 2 (A) Bright field image of a section of the main channel loaded with L1210 cells. Shown here are 245 cells on 304 holes (80% loaded). (B) Fraction of occupied holes over time. Initially, after insecurely-trapped cells are rinsed away, 64% of the imaged holes are occupied by cells. Over time, however, newborn cells are captured by nearby empty holes, such that eventually over 90% of the holes are occupied.

device, with most holes trapping a single cell. Since the loading mechanism is an active pressure differential rather than a passive settling probability, a large fraction (60–80%) of the imaged holes is occupied by cells after rinsing away insecurely-captured cells. In addition, the fraction of occupied holes generally increases over time as newborn cells are caught onto empty neighboring holes (Fig. 2b). However, not all of the holes end up capturing a cell because some may be obstructed by debris. The steady fraction of loaded holes achieved over time indicates that cells rarely come unstuck from the holes, preventing contamination of the eluted cells with non-newborn cells.

The loaded cells then remain on the device to grow and divide over time, as shown in Fig. 3a (also see supplementary movie†). Although only a subset of images is shown, cells were observed to grow and divide on chip for the complete duration of the experiment (3 days). Next, to assess the health of the cells growing in the device, the mean interdivision time of the cells seen in time-lapse images was compared to the cell doubling time in culture. The interdivision time was taken as the time from the beginning of one cytokinesis to the beginning of the next

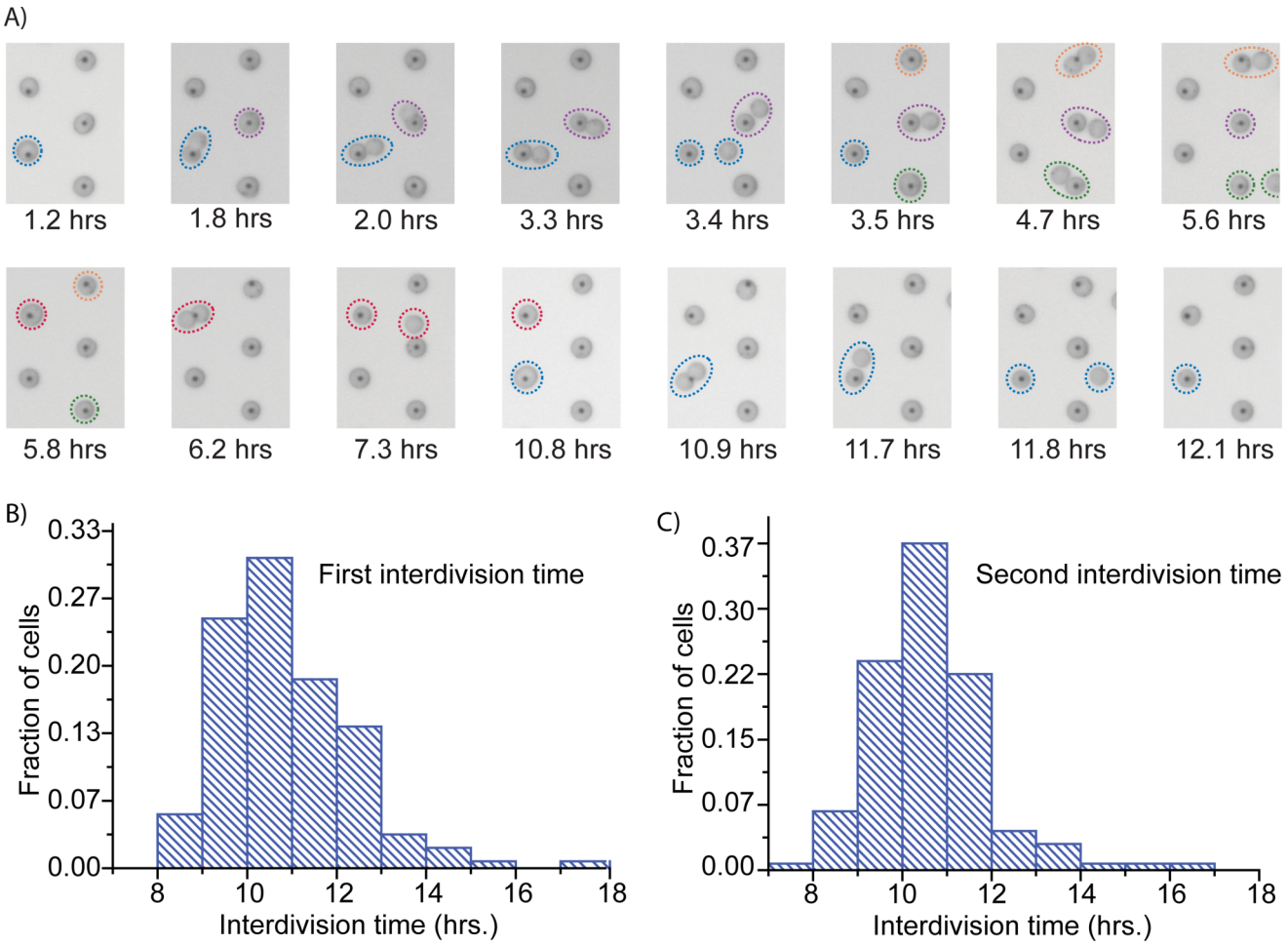

Fig. 3 (A) Time-lapse images of five cells growing and dividing on the device. The time denoted below each image indicates elapsed time after the device had been loaded with cells and rinsed to remove any unattached cells. Fluid flow is from left to right. Colored dotted circles track cytokinesis followed by separation and release of a newly divided cell. Note that the bottom left cell (circled in blue) divides twice within the given time frame. (B) Distribution of the first interdivision time of cells growing in the device, counted from the initial signs of pinching during the first division to the initial signs of pinching during the second division, as captured by time-lapse images (5 min per frame). N = 150 cells, median = 10.8 h, mean = 10.9 h, standard dev. = 1.5 h. (C) Distribution of the second interdivision time, taken as the time between the second and third division using the same method as in (B). N = 135 cells, median = 10.4 h, mean = 10.6 h, standard dev. = 1.3 h. The mean interdivision times through both divisions correspond well to the observed doubling time of the cells grown in bulk culture (10–11 h).

cytokinesis. Fig. 3b and c display the interdivision times of two consecutive division cycles for cells docked on the trapping holes. The mean interdivision times of 10.8 h (between the first and second divisions) and 10.6 h (between the second and third divisions) are comparable to the 10–11 h doubling time observed in culture, and also agree well with the times given in previous studies.[29,34] The reduction in the reported number of second interdivision times is mainly due to some cells dividing while not being imaged, and other cells slipping through the trapping holes either because of the pliability of the cells or differences in hole sizes caused by variations in the microfabrication process. The results indicate that cells can grow and divide well on chip under the constant perfusion of media.

Yield and synchrony

After validating cell growth in the device, the output of the microfluidic "baby machine" was assessed to determine the yield and synchrony of the eluted cells. Fig. 4a depicts the number of cells collected at each 12 hour time point. The initial increase in cell count between the first two time points corresponds with the fact that not all of the trapping holes are filled with cells initially, and as the trapped cells divide, some of the newborn cells are caught onto nearby vacant holes rather than being eluted from the device (Fig. 2b). Then, from 24 to 36 h, the number of cells outputted plateaus at $\sim$1000 cells every 12 h. Based on the number of cells in the device and their doubling time, the output may be lower than expected. Although not affecting the health of the cells, causes for lower yield may include imprecision in estimating the total number of cells on the device and in the collection chamber, as well as loss of cells in the gasket interface. Furthermore, some cells slip through the trapping holes after having been docked, allowing newborn cells to occupy the recently vacated holes, which then lowers the overall yield of the device. In spite of this, the output reaches a steady value and the cells are not only growing in the device, but also dividing and producing new cells for at least 36 h of device operation.

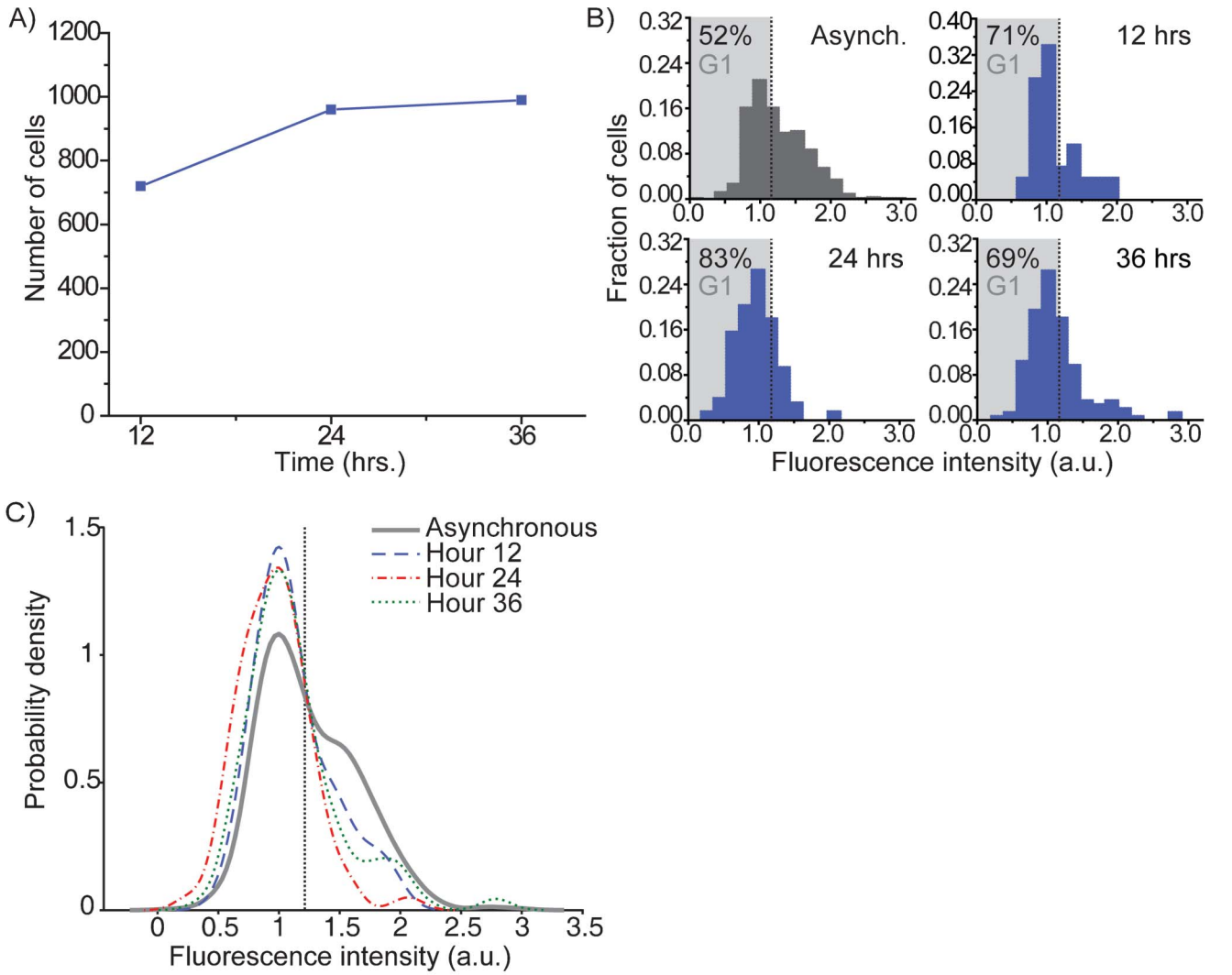

Fig. 4 (A) Yield from the device over time. Synchronized cells were eluted into a formaldehyde fixative and fractions were collected and counted every 12 h. Note that the system produces a steady output from 24 to 36 h. (B) DAPI fluorescence intensity distributions for each 12 hour fraction. The control population is an asynchronous population of cells taken from bulk culture. At each time point a threshold of 1.2 fluorescence intensity units is set to estimate the fraction of cells corresponding to G1 DNA content, as indicated by the percentages written in each shaded region. N = 677, 41, 128, and 144 cells, for the asynchronous, 12, 24, and 36 hour time points, respectively. (C) Kernel density estimates of DAPI intensity distributions for each time point, overlaid with that of the asynchronous control. The dotted vertical line marks the 1.2 unit threshold. In all cases, the fluorescence intensity data is normalized such that the G1 modal value is at 1.0 units. The right shoulder in the control data, corresponding to DNA content of cells in G2/M, is clearly diminished for the fractions taken at the output of the device. Also note the increased probability density of the G1 peaks of the device output (dashed lines) compared to the asynchronous population (solid line), indicating synchrony in G1.

Also at each 12 hour time point, the fixed fractions of eluted cells were stained with DAPI to evaluate the distribution of DNA content. In Fig. 4b, the cells' fluorescence intensities were normalized such that the G1 DNA content distribution has a modal value of 1.0 unit. Based on the distribution of the control data taken from an asynchronous population of cells, a threshold was set at 1.2 units, corresponding to one standard deviation above the mean of a Gaussian curve fitted to the G1 peak. Cells with a fluorescence intensity less than this value (indicated by the shaded regions in Fig. 4b) are considered to be in G1 phase, while values above the threshold correspond to cells in S/G2/M. The G2/M peak falls at an intensity less than 2.0 units, most likely due to chromatin packing during G2 and formaldehyde induced cross-linking that may have hindered the access of the dye to DNA binding sites.[35] For an asynchronous, exponentially-growing control population, 52% of the cells have a DAPI intensity of less than 1.2 units (and thus are in G1). Within the first 36 h of operation, a purity of up to 83% of the cells having G1 DNA content was obtained from our microfluidic "baby machine".

Next, a Kolmogorov–Smirnov test was carried out to compare the fraction at each time point to the control population. The null hypothesis was rejected each time, having p-values of 0.026, 9.1×10^{-10}, and 1.8×10^{-4} at the 12, 24, and 36 hour time points, respectively. Hence, the cells being outputted from the microfluidic "baby machine" have a significantly different DNA content distribution than the asynchronous control population. From the overlaid kernel density estimates shown in Fig. 4c, it is

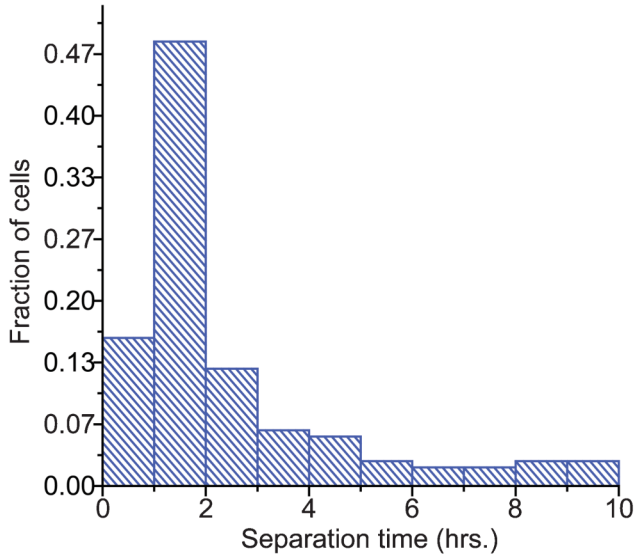

Fig. 5 Time for a cell to separate from its sister cell after morphological signs of a cleavage furrow are evident, taken from time lapse images (5 min per frame). $N = 150$ cells, median = 1.6 h, mean = 2.2 h, standard dev. = 2.0 h. 83% of the cells fully detached from its sister cell within 4 h, including time for cytokinesis.

clear that at all of the time points the probability density of the G1 peak increased, while the G2/M shoulder diminished compared to the asynchronous population, suggesting a largely synchronous population of cells in G1.

Additional information regarding the age of the cells was garnered from bright field time-lapse images. The elapsed time from the appearance of a cleavage furrow during cytokinesis until the cells fully separate and one disappears from the field of view was calculated, and the distribution of these times is shown in Fig. 5. The median amount of time for cells to separate is 1.6 h. Note that this time includes the time for cytokinesis. Here, 83% of the cells separated within 4 h of beginning cytokinesis. This means that at least 83% of cells were collected in G1 phase, since G1 phase (not including cytokinesis time) for L1210 cells should be 4–5 h according to data reported in the literature.[36] The similarity between the fraction of G1 cells estimated by separation time and that obtained by DAPI staining indicates that the purity of synchrony is partly affected by inherent biological variation in cytokinesis and cell separation. This variation would also affect previous baby machines, which have been shown to maintain synchrony over many divisions.[29] In summary, according to both DAPI staining and separation times calculated from time-lapse imaging, over 80% of the eluted cells are in G1 phase.

Conclusions

The presented cell synchronization device serves to demonstrate the principle of a pressure-controlled baby machine. Rather than using surface chemistries to adhere cells to a membrane, the microfluidic device successfully uses pressure differences across trapping holes and fluidic ports to capture cells on the device, allow them to grow and divide, and elute newborn cells that have entered the G1 phase of the cell cycle. On a device with 2109 holes, up to 1000 cells are eluted every 12 h, with a purity of up to over 80% of the collected cells being in G1.

Although the device presented here is functional, a few deficiencies will need to be addressed in future versions of the microfluidic "baby machine". First, it was difficult to confirm the clearing of all the trapping holes while cleaning the device before reuse. Obstructed holes may hinder proper loading of cells and lower the overall yield of the device, although not necessarily altering its synchronizing functionality. Second, even after lengthy device preparation times, it was difficult to ensure the removal of all air bubbles beneath the trapping holes. Over long runs, these bubbles can expand and dislodge loaded cells. Third, beyond 36 h of operation, aggregates of cells can form in the trapping chamber and occasionally detach from the surface, releasing non-newborn cells from the device. In spite of this, the current 36 hour window of operation may be sufficient for many biological experiments, which require only a single synchronized batch of cells and not a continuous supply.

The current yield of the synchronization device is sufficient as a demonstration and possibly for transcriptomic analysis, but would need to be greatly increased for investigations on the level of protein expression. To this end, it should be feasible to stack these 2-dimensional devices into a 3-dimensional array of trapping holes, thereby vastly increasing the yield of the device. Hence, there remains further development to improve the operation and increase the yield of the microfluidic "baby machine". As a demonstrated concept, however, since the presented technique avoids damaging chemicals, selects for age rather than size, and does not depend on surface properties of cells, it may prove to be a less perturbing and more versatile way to synchronize cells.

Acknowledgements

We thank Amneet Gulati and Nathan Cermak for valuable discussions and guidance with statistical analysis. We also thank Marc Kirschner and Amit Tzur at Harvard Medical School for valuable discussions and for providing L1210 mouse lymphocytic leukemia cells. Devices were fabricated through the use of the Microsystems Technology Laboratories at the Massachusetts Institute of Technology. This work was supported by the National Cancer Institute Physical Sciences Oncology Center U54CA143874 as well as the National Institute of General Medical Sciences (NIGMS) EUREKA R01GM085457.

References

1 E. Hernando, *et al.*, *Nature*, 2004, **430**, 797–802.
2 H. Y. Chang, *et al.*, *PLoS Biol.*, 2004, **2**, 206–214.
3 M. L. Whitfield, L. K. George, G. D. Grant and C. M. Perou, *Nat. Rev. Cancer*, 2006, **6**, 99–106.
4 W. A. Kues, M. Anger, J. W. Carnwath, D. Paul, J. Motlik and H. Niemann, *Biol. Reprod.*, 2000, **62**, 412–419.
5 G. F. Merrill, *Methods Cell Biol.*, 1998, 229–249.
6 G. Banfalvi, *Cell Cycle Synchronization*, 2011, 1–23.
7 R. E. Uzbekov, *Biochemistry (Moscow)*, 2004, **69**, 485–496.
8 A. Kurose, T. Tanaka, X. Huang, F. Traganos and Z. Darzynkiewicz, *Cell Proliferation*, 2006, **39**, 231–240.
9 Z. Darzynkiewicz, H. D. Halicka, H. Zhao and M. Podhorecka, *Cell Cycle Synchronization*, 2011, 85–96.
10 C. J. Li and T. H. Elsasser, *Journal of Animal and Veterinary Advances*, 2006, **5**, 916–923.

11 F. H. Kasten, F. F. Strasser and M. Turner, *Nature*, 1965, **207**, 161–164.
12 D. J. Grdina, M. L. Meistrich, R. E. Meyn, T. S. Johnson and R. A. White, *Techniques in Cell Cycle Analysis*, 1987, 367–402.
13 S. Cooper, *Trends Biotechnol.*, 2004, **22**, 266–269.
14 P. T. Spellman and G. Sherlock, *Trends Biotechnol.*, 2004, **22**, 270–273.
15 S. Cooper, *Trends Biotechnol.*, 2004, **22**, 274–276.
16 J. Gong, F. Traganos and Z. Darzynkiewicz, *Cell Growth & Differentiation*, 1995, **6**, 1485–1493.
17 P. E. Lindahl, *Nature*, 1948, **161**, 648–649.
18 P. E. Lindahl, *Biochim. Biophys. Acta*, 1956, **21**, 411–415.
19 G. Banfalvi, *Nat. Protoc.*, 2008, **3**, 663–673.
20 U. Kim, C.-W. Shu, K. Y. Dane, P. S. Daugherty, J. Y. J. Wang and H. T. Soh, *Proc. Natl. Acad. Sci. U. S. A.*, 2007, **104**, 20708–20712.
21 P. Thevoz, J. D. Adams, H. Shea, H. Bruus and H. T. Soh, *Anal. Chem.*, 2010, **82**, 3094–3098.
22 S. Choi, S. Song, C. Choi and J.-K. Park, *Anal. Chem.*, 2009, **81**, 1964–1968.
23 S. Migita, K. Funakoshi, D. Tsuya, T. Yamazaki, A. Taniguchi, Y. Sugimoto, N. Hanagata and T. Ikoma, *Anal. Methods*, 2010, **2**, 657–660.
24 W. C. Lee, A. A. S. Bhagat, S. Huang, K. J. Van Vliet, J. Han and C. T. Lim, *Lab Chip*, 2011, **11**, 1359–1367.
25 G. Cooper, *The Cell: A Molecular Approach*, 2000, 592.
26 M. H. Fox, R. A. Read and J. S. Bedford, *Cytometry*, 1987, **8**, 315–20.
27 M. H. Fox, *Cell Cycle Checkpoint Control Protocols*, 2004, **241**, 11–16.
28 C. E. Helmstetter and D. J. Cummings, *Proc. Natl. Acad. Sci. U. S. A.*, 1963, **50**, 767–774.
29 M. Thornton, K. L. Eward and C. E. Helmstetter, *BioTechniques*, 2002, **32**, 1098–1105.
30 V. S. Lebleu, M. Thornton, S. R. Gonda and C. E. Helmstetter, *Cytotechnology*, 2006, **51**, 149–157.
31 D. M. Wang and J. M. Tarbell, *J. Biomech. Eng.*, 1995, **117**, 358–363.
32 A. M. Malek, S. L. Alper and S. Izumo, *J. Am. Med. Assoc.*, 1999, **282**, 2035–2042.
33 T. N. Siegel, D. R. Hekstra and G. A. M. Cross, *Mol. Biochem. Parasitol.*, 2008, **160**, 171–174.
34 A. Tzur, R. Kafri, V. S. LeBleu, G. Lahav and M. W. Kirschner, *Science*, 2009, **325**, 167–171.
35 J. C. S. Wood and P. Todd, *Cell Biophys.*, 1979, **1**, 211–218.
36 S. Cooper, *Cell Biol. Int.*, 2002, **26**, 715–727.